Temperature (208-318 K) and pressure (18-696 Torr) dependent rate coefficients for the reaction between OH and HNO$_3$.

Katrin Dulitz[1,a], Damien Amedro[1], Terry J. Dillon[1,b], Andrea Pozzer[1], and John N Crowley[1]

[1] Division of Atmospheric Chemistry, Max-Planck-Institut für Chemie, 55128 Mainz, Germany

5   [a] now at: Nanophysics research group, University of Freiburg, 79104 Freiburg, Germany

[b] now at: Department of Chemistry, University of York, York, U.K

Supplementary Information

Table S1: Experimental rate coefficients, k_5

T (K)	p (Torr)	k_5	HNO$_3$	T (K)	p (Torr)	k_5	HNO$_3$	T (K)	p (Torr)	k_5	HNO$_3$
208	20.0	6.30 ± 0.29	a	242	496.0	3.66 ± 0.07	a	275	50.0	$1.68 \pm 0.02^*$	w
217	20.0	4.61 ± 0.06	a	242	529.7	3.66 ± 0.05	w	275	50.0	1.61 ± 0.02	w
217	20.0	4.81 ± 0.05	a	242	530.5	3.55 ± 0.06	a	277	99.3	1.75 ± 0.02	t
218	50.0	5.58 ± 0.05	a	245	294.1	3.12 ± 0.06	w	276	98.6	1.76 ± 0.02	a
217	50.0	6.13 ± 0.12	a	245	294.9	3.09 ± 0.07	w	276	99.4	1.77 ± 0.02	w
217	91.1	6.46 ± 0.10	a	245	295.1	3.23 ± 0.05	w	277	121.2	1.74 ± 0.02	t
227	20.0	4.08 ± 0.04	a	245	295.8	3.09 ± 0.05	w	278	196.3	1.71 ± 0.02	t
227	20.9	3.96 ± 0.03	a	245	296.4	3.23 ± 0.05	a	278	196.4	1.75 ± 0.03	t
227	50.2	4.72 ± 0.05	a	246	493.5	3.23 ± 0.07	w	278	285.0	1.77 ± 0.01	w
227	146.1	5.13 ± 0.10	a	257	20.0	2.00 ± 0.02	a	278	296.0	1.77 ± 0.03	t
227	296.1	5.46 ± 0.21	a	257	23.7	2.14 ± 0.02	w	278	296.8	1.78 ± 0.02	a
227	495.9	5.84 ± 0.18	a	257	50.0	2.23 ± 0.02	a	277	398.2	1.75 ± 0.02	t
239	17.7	3.09 ± 0.03	w	257	99.9	2.41 ± 0.02	w	276	500.9	1.82 ± 0.02	w
239	17.9	3.01 ± 0.03	w	257	300.1	2.55 ± 0.03	a	275	601.8	1.84 ± 0.02	w
239	18.2	3.07 ± 0.05	w	257	300.6	2.54 ± 0.03	w	297	18.1	1.26 ± 0.02	a
239	19.5	3.09 ± 0.07	w	257	400.8	2.54 ± 0.03	w	297	20.0	$1.23 \pm 0.01^*$	w
239	49.4	3.54 ± 0.03	w	257	499.3	2.48 ± 0.04	a	297	27.3	1.24 ± 0.01	w
239	49.8	3.54 ± 0.06	w	257	562.5	2.56 ± 0.03	w	297	50.0	1.29 ± 0.01	w
239	49.8	3.53 ± 0.03	w	276	17.9	1.59 ± 0.02	a	297	98.7	1.35 ± 0.02	a
239	50.1	3.53 ± 0.04	a	276	18.2	1.69 ± 0.03	t	298	220.5	1.38 ± 0.01	t
239	50.2	3.61 ± 0.04	w	276	18.2	1.67 ± 0.02	t	297	296.3	1.40 ± 0.02	t
239	49.7	3.40 ± 0.04	w	276	18.3	1.60 ± 0.02	w	297	301.2	1.36 ± 0.01	w
242	20.0	2.74 ± 0.04	a	275	20.0	$1.56 \pm 0.02^*$	w	298	396.6	1.40 ± 0.01	t
242	22.3	2.81 ± 0.02	w	275	20.0	1.60 ± 0.02	w	297	500.6	1.38 ± 0.01	w
242	50.2	3.19 ± 0.05	a	276	25.3	1.62 ± 0.01	w	297	650.2	1.39 ± 0.02	w
242	99.0	3.40 ± 0.05	w	276	35.1	1.67 ± 0.01	t	318	29.2	1.05 ± 0.01	w
242	99.2	3.47 ± 0.04	w	275	35.4	1.71 ± 0.02	t	319	696.1	1.12 ± 0.01	w
242	146.1	3.54 ± 0.05	a	275	36.2	1.71 ± 0.02	t				
242	296.3	3.63 ± 0.07	a	275	40.1	1.68 ± 0.01	a				

10   Units of k_5 are 10^{-13} cm^3 molecule^{-1} s^{-1}, measurements in synthetic air are marked with an asterisk, errors are statistical only (two standard deviations); abbreviations: a = anhydrous HNO$_3$, w = 90 % HNO$_3$, t = ternary mixture

TPEFS detection of HNO₃: Correction of data due to fluorescence quenching and absorption of excitation light by HNO₃.

In this section, we describe in detail the method used to correct the TPEFS signal as a function of [HNO₃]. At high HNO₃ concentrations ($>10^{14}$ cm^{-3}) relevant for this study, 193 nm light absorption between the entrance Brewster window and the excitation volume at the centre of the reactor can reduce the rate of dissociation of HNO₃ to HONO* and also the dissociative excitation of HONO*, thus reducing sensitivity. In addition, the quenching of OH fluorescence by large concentrations of HNO₃ can also act in the same direction, both effects resulting in a non- linear response of TPEFS as a function of [HNO₃] as exemplified in Fig. S1, which displays the variation of the TPEFS signal with [HNO₃] at two different total pressures. Even though we were able to parametrize the TPEFS signal over a wide range of [HNO₃] (up to 10^{16} molecule cm^{-3}) and pressures (25 to 150 Torr N₂) we performed most of these experiments at constant [HNO₃] and densities to simplify the analysis.
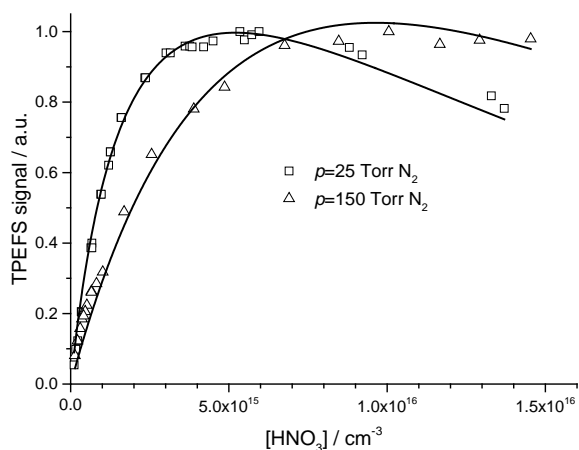
Figure S1. Dependence of the TPEFS signal on [HNO₃] at p=25 and 150 Torr N₂ at room temperature. Solid lines corresponds to a global fit using eq. (S1) where l = 5 cm (fixed), k_{N2}=1.3 10^{-11} cm^3 molecule^{-1} s^{-1} (fixed) and k_{HNO3}=5.4 10^{-9} cm^3 molecule^{-1} s^{-1} (varied).

The TPEFS signal is given by the following expression,

$$S_{TPEFS} = C \cdot N \cdot \frac{I}{I_0} \cdot [\text{HNO}_3] \cdot \phi \tag{1}$$

Where C is a calibration factor (dependent on PMT characteristics, fluorescence collection efficiency etc.), N is the photon density in photon/cm^2, I / I_0 is the fraction of the 193 nm photons that reach the centre of the reaction cell:

$$\frac{I}{I_0} = e^{-(\sigma_{193nm}[\text{HNO}_3]l)} \tag{2}$$

where $\sigma_{193\ nm}$ is the cross-section of HNO_3 at 193 nm (1.15×10^{-17} cm^2 molecule^{-1})[8], l is the absorption length in cm and ϕ is the fluorescence yield:

$$\phi = \frac{kf}{kf + k_{N2}[N_2] + k_{HNO3}[HNO_3]} \qquad (3)$$

where k_f is the OH fluorescence rate constant in s^{-1} ($1.5\ 10^6$ s^{-1}) (German, 1975), k_{N2} and k_{HNO3} are the quenching rate coefficient (in cm^3 molecule^{-1} s^{-1}) of N_2 and HNO_3 respectively.

Of the parameters given above, the absorption length and the quenching rate coefficients for N_2 and HNO_3 needed to be determined. We measured the absorption length by recording the 193 nm light attenuation as a function of [HNO_3] (see Figure S3) using a Joule meter placed at the rear of the reactor. The Joule meter signal as a function of [HNO_3] was fitted to the Beer-Lambert law (eq. 2) and an absorption length of $\approx$ 10 cm was obtained. The fluorescence is detected in the middle of the reactor and so the absorption length l in eq. (1) is $\approx$ 5 cm.
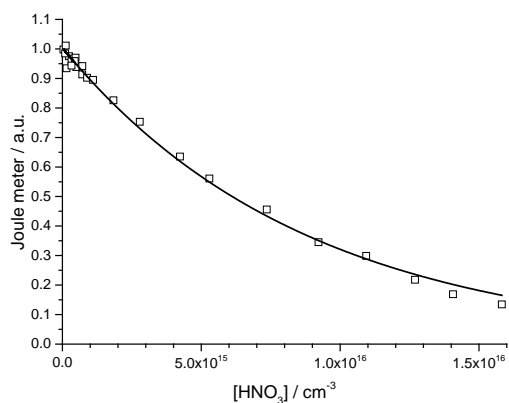
Figure S2. Extinction of 193 nm light by [HNO_3]. The effective path-length for absorption was calculated using the literature cross-section of HNO_3 at 193 nm.

The rate constant for OH(A) quenching by N_2 (k_{N2}), determined by varying the N_2 pressure at constant HNO_3 concentration at room temperature, was found to be 1.3×10^{-11} cm^3 molecule^{-1} s^{-1}, which is in excellent agreement with Kenner et al. (1986).

The rate constant for OH(A) quenching by HNO_3 (k_{HNO3}) is reported to be 5.9×10^{-10} cm^3 molecule^{-1} s^{-1} (Kenner et al., 1986). Using these parameters does however not reproduce the strong HNO_3 dependence at [HNO_3]$> 10^{15}$ cm^{-3} and a value of k_{HNO3} of 5.4×10^{-9} cm^3 molecule^{-1} s^{-1} better reproduces our observations. The difference between the value we require to match our observations and the literature rate constant for k_{HNO3} indicates that the expression used here to describe the TPEFS signal as a function of [HNO_3] is an approximation that does not include for example the effect of N_2 and HNO_3 on the energy transfer from highly excited vibrational states of the first electronic state down to OH(A) v'=0. Also, we simplified the expression to a one-absorption phenomenon where OH(A) is actually the result of a 2-photon sequential

absorption process. The parametrized expression is however sufficient to reproduce our experimentally observed dependence of the TPEFS signal on [HNO_3] (see Figure S1).

We also explored the temperature dependence of the N_2 quenching rate of OH(A) in an experiment with constant [HNO_3] and constant [N_2]. The first order decay constant for the OH fluorescence was derived by fitting a single exponential decay to the raw signal recorded by a 100 MHz oscilloscope.

We found no significant change in the OH fluorescence decay rate as we lowered the temperature (see Figure S3), which contrasts the weak dependence observed for OH quenching from (A, v´=0) due to collisions with N_2 (dashed line in Figure S4) (Copeland and Crosley, 1986). The difference is likely related to the fact that nascent OH generated in the two-photon excitation of HNO_3 is very hot, with an approximate vibrational temperature of 3200 K and rotational temperature of 700 K. As the required rate constant for quenching by HNO_3 exceeds 10^{-9} cm^3 molecule^{-1} s^{-1}, we assume that this parameter is, to a good approximation, independent of temperature.
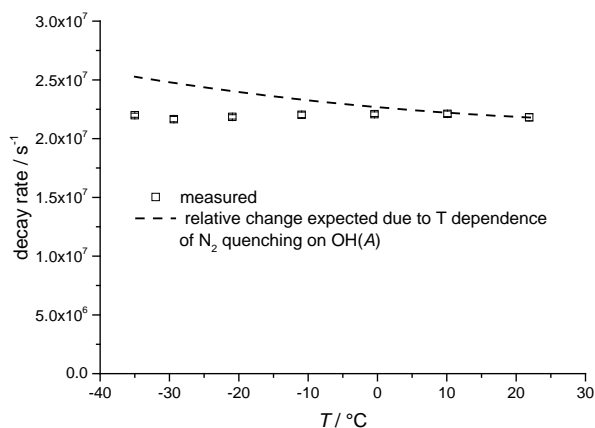
Figure S3. OH fluorescence decay rate as a function of temperature. Conditions: pressure = 50 Torr N_2 and [HNO_3] = 2.7 10^{15} molecule cm^{-3}

References

Kenner, R. D., Rohrer, F., Papenbrock, T., and Stuhl, F.: Excitation mechanism for OH(A) in the ArF excimer laser photolysis of nitric acid. J. Phys. Chem., 90, 1294-1299, doi:10.1021/j100398a018, 1986.
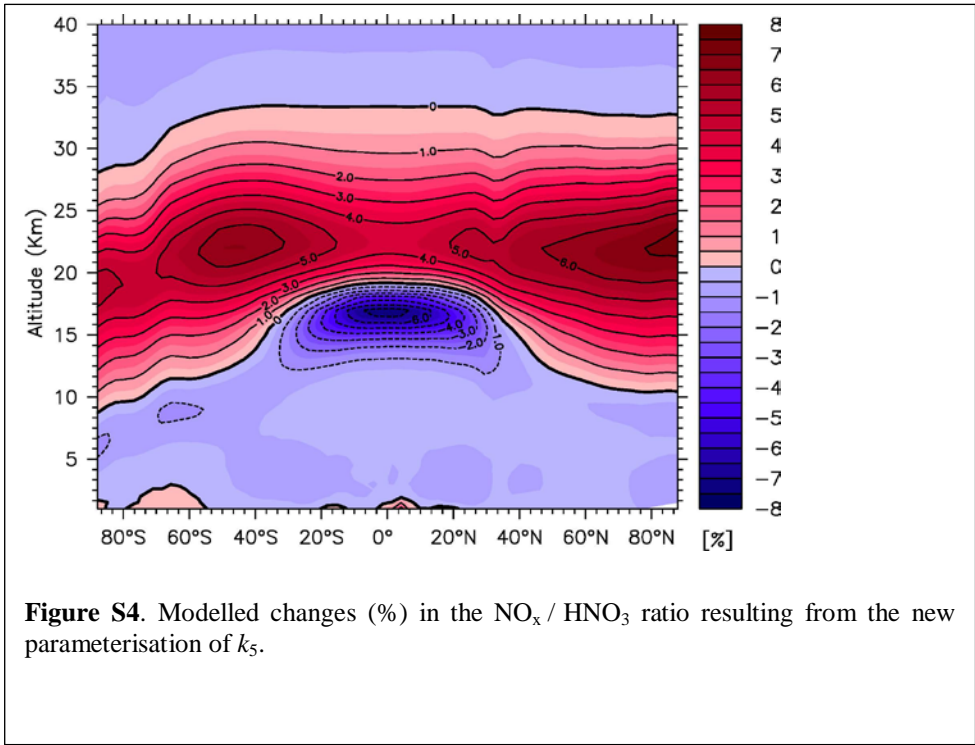
Figure S4. Modelled changes (%) in the NO_x / HNO_3 ratio resulting from the new parameterisation of k_5.